Bluetooth Low Energy Communication for Multi-Sensor Applications Design and Analysis

by

João Pedro Tavares Mendonça Garretto

Submitted in Partial Fulfillment of the Requirements

for the Degree of

Master of Science in Engineering

in the

Electrical and Computer Engineering

Program

YOUNGSTOWN STATE UNIVERSITY

December 2022

Bluetooth Low Energy Communication for Multi-Sensor Applications Design and Analysis

João Pedro Tavares Mendonça Garretto

I hereby release this thesis to the public. I understand that this thesis will be made available from the OhioLINK ETD Center and the Maag Library Circulation Desk for public access. I also authorize the University or other individuals to make copies of this thesis as needed for scholarly research.

Signature:

João Pedro Tavares Mendonça Garretto, Student Date

Approvals:

Dr. Frank X. Li, Thesis Advisor Date

Dr. Pedro Cortes, Committee Member Date

Dr. Vamsi Borra, Committee Member Date

Dr. Salvatore A. Sanders, Dean of Graduate Studies Date

Abstract

Bluetooth Low Energy (BLE) has emerged as one of the main wireless technologies used in low-power electronics, such as wearables, beacons, and devices for the Internet of Things (IoT). BLE's energy efficiency characteristics and ease of use interface are essential features for the design of ultralow-power devices. The integration of BLE with various sensors is certainly the main aspect for the development of efficient solutions, and monitoring the power consumption of the device in all the cycles of operation is important for decisions such as advertising interval, sensor routine and data transmission.

Recent work of BLE power analysis focuses on the theoretical aspects of the advertising and scanning cycles, with most results being presented in the forms of mathematical models and computer software simulations. Such models and simulations are particularly important for the understanding of the technology. However, many times they leave real applications out of scope.

This thesis covers the implementation of a multi-sensor Bluetooth Low Energy system, and the study of the communication protocol regarding its power consumption and RF performance. The implementation consists of a battery powered custom Printed Circuit Board (PCB) featuring the Texas Instruments CC1352P7 as the main SoC and three different sensors capable of measuring 6 different parameters. The sensors are the BME688 from Bosch, and the ADXL343 and AD5941 from Analog Devices. The characterization process was performed using Keysight EXR Oscilloscope and 208A Spectrum Analyzer.

The proposed design has dimensions of 28 mm × 35 mm. The current consumption of the implemented design with one sensor in operation is 4.1mA and 7.1mA, and 6.9 mA combined.

Contents

Table of Figures

Acknowledgement

As I conclude my journey at Youngstown State University (YSU), I must demonstrate gratitude to everyone that has helped me along the way.

First, I would like to thank my advisor Dr. Frank X. Li, for trusting me with the opportunity to undertake this project, for his guidance and support on technical aspects, and for his innumerable advices and mentorship. I would also like to thank Dr. Vamsi Borra and Dr Pedro Cortes for their support in these past eighteen months, and their contributions and constructive feedback on this work.

Secondly, thank you to all my classmates and lab partners for all their support and for making the daily routine on the 3rd floor of Moser Hall fun and enjoyable. I would also like to thank the remaining YSU Electrical Engineering faculty for all the knowledge shared with me and for enabling key learning opportunities.

Last but not least, I would like to thank my family. Your support and love were felt every day, and I'm sure it made the whole difference in the end. Thank you for always encouraging me in the good and bad days.

C. S. S. M. L.

1. Introduction

Over the last year at YSU, researchers from different faculty and departments were looking for a better method to collect data from their experiments. Therefore, a wireless data acquisition device scalable to various applications was idealized to fulfill such demand. The intended design would not only serve for data collection of current research but also as a base platform for future work, where small modifications in hardware and software would have to be made to fulfil data collection goals.

Recently, technologies such as Wi-Fi, ZigBee, Bluetooth Classic and Bluetooth Low Energy (BLE) emerged to fulfill the constant need for wireless connectivity. The integration of IoT devices with legacy industrial systems, as well as the constant development of wearable technologies and smart systems are a few of the many applications supported by such wireless protocols [1]. Each technology possesses its own advantages and disadvantages, for instance, ZigBee, is intended to provide, low-cost, low-power, and easy-to-install and maintain wireless connectivity for low data-rate monitoring applications but presents difficulties regarding connections with smartphone applications. Wi-Fi technology offers high data transmission, but also greater power consumption, and like ZigBee is inconvenient with respect to device connection and smartphone applications development [2]. BLE stands out as a low-power and a secure alternative with communication that makes it easy to interface with different devices and cell phone applications [3]. After careful revision, it was decided that the system would use BLE as its main protocol.

Upon initializing the design, and reviewing the current literature on BLE systems, it was noted the extensive work on the new applications enabled by the technology, and how the power consumption was always a particularly crucial point in the final evaluation of each device. However, while performing in depth research exclusively in power analysis, it was clear that most

literature involved the development of new mathematical models and computer simulations on how to optimize the advertising cycle and processes behind it, often leaving real measurements and applications out of the scope.

The work presented in this thesis intends to detail the hardware design of a multi-sensor Bluetooth Low Energy system, while providing in-depth analysis of its energy consumption. Serving as a base for future designers to leverage wireless applications by better understanding BLE's power performance and characteristics in different scenarios.

2. Literature Review

2.1. Previous Work

As BLE was designed to significantly reduce power consumption and improve interoperability between devices, a lot of research has been enabled by using BLE as the technology responsible for the wireless communications, increasing the number of applications and tasks for systems with low-power requirements. Also, standalone investigations using the current consumption of a BLE system are made to track BLE events and model optimizations and novel methods to improve the efficiency of such devices.

The role of IoT devices in rural applications has certainly increased with BLE, a sensor node for animal monitoring was designed and evaluated with regards to its power consumption [4]. In that study, researchers focused on an ultra-low power device intended to monitor the jaw activities of cattle, where an accelerometer tracks the movement of the animal and evaluates its behavior based on the data transmitted via BLE. A performance evaluation is completed with results of the current consumption of the device while using advertising time-interval, as well as while the sensor node is connected to another device.

Taskin *et al.* [5] designed a sensor node for IoT applications in agriculture. The system has ambient light and temperature sensors used to monitor such parameters in a greenhouse. Later, the paper also investigates the power consumption of the sensor node in different conditions such as stand-by mode and when in full operation with the sensors and analyses the management cost per hectare. Concluding that the low cost of the design is extremely attractive for improvements in farming operation.

Healthcare monitoring has been enabled by the low-power consumption of BLE, the related research is a design of a battery powered wearable medical sensor network capable of monitoring

vital signs such as heart rate, respiration rate and body temperature that uses a separate BLE transceiver as the wireless technology of the system [6][7]. Sabatini *et al.* [8], in an equivalent way, proposed a system capable of evaluating the anaerobic threshold analyzing only samples of saliva and exhaled breath to examine athletic performances with a non-invasive technique. The sensor data is transmitted via BLE to smart devices. The final power consumption is 80mW, enabling the system to operate for a long time in different modalities.

Dian *et al.* [9], expands the idea of using current measurement patterns as a means for time synchronization purposes among BLE devices, where the monitoring of a set of events that occur at the same time can be used for time synchronization. In the paper, the current consumption pattern of BLE is also explained. In another paper Dian *et al.* [10] evaluate the performance of the time synchronization BLE strategy developed in [9]. The performance is evaluated in terms of several parameters such as number of nodes, workload of BLE processor, workload of main processor and distance. In [11] Dian proposes an architecture for a multichannel DAQ device communication system based on BLE protocol. The system is composed of a BLE master node, which is connected to database, and BLE slave nodes that have the sensors collecting data and focus on time synchronization to achieve a design that is energy efficient and provides relatively long range for the Bluetooth technology.

Expanding on the research of BLE current consumption and power analysis, Liu *et al.* [12] presented a quantitative analysis on the neighbor discovery energy pattern of BLE. The analytical model is proposed to analyze the expectation of the energy consumption in the process, which is then validated with an extensive set of experiments. The paper concludes with insights on timing set up for determined parts of the BLE advertising cycle and its influence on the current consumption.

As BLE is employed in many continuous data collection applications, any improvements in the energy consumption translates to larger battery live time and applicability. Feng *et al.* [2] proposes a strategy to efficiently reduce the energy consumption of continuous data transmission on BLE. The method aims to cut down the transmission average current by changing the size of sensor data packet in the same sampling frequency of sensors. Results show that the method works and that the average transmission current is reduced.

2.2. Bluetooth Low Energy

This section presents an overview of the Bluetooth Low Energy (BLE) history and technology, including its radio frequency operating band, range, protocol structure and how the communication works.

The development of Bluetooth technology started by the Bluetooth Special Interested Group (SIG) as an early exploration to achieve short-range communications, its foundation core uses the Frequency Hoping Spread Spectrum (FHSS) technology, and the first version was released in 1999. From 2004 to 2009, newer versions of Bluetooth technology were developed, known as Bluetooth Classic. Such versions operate with a radio that streams data over seventy-nine channels, each with 1 MHz, starting at the 2.4GHz unlicensed industrial, scientific, and medical (ISM) frequency band, and has a bit rate of 1, 2 and 3 Megabits per second. [1][3][9]

In 2010, Bluetooth SIG released an innovative technology named Bluetooth Low Energy, which is equivalent to Bluetooth 4.0. BLE radio is designed for extremely low-power operation and operates at the 2.4GHz ISM band, however, unlike Bluetooth Classic, it transmits data over forty channels of 2 MHz, and bit rate of 1Mbps with an option of 2Mbps in Bluetooth 5. It also has three channels dedicated exclusively to advertising. Over the years, newer versions of BLE have been released, the latest one being Bluetooth 5.2. [3][9]

The BLE protocol structure, shown in Figure 1, is composed of a stack with three main blocks, the Application, the highest block of the stack, and the layer that direct interface with the user, the Host, and the Controller which are the main components of the BLE protocol and have different layers, each responsible for a particular function in the BLE operation. [3][9]

<table>
<tr><td>Application Layer</td><td colspan="2">Application/Profiles</td></tr>
<tr><td rowspan="4">BLE Host Layer</td><td colspan="2">Generic Access Profiles (GAP)</td></tr>
<tr><td colspan="2">Generic Attribute Profile</td></tr>
<tr><td>Security Manager (SM)</td><td>Attribute Protocol (ATT)</td></tr>
<tr><td colspan="2">Logical Lingk Control and Adaption Protocal (L2CAP)</td></tr>
<tr><td></td><td colspan="2">Host Controller Interface (HCI)</td></tr>
<tr><td rowspan="2">BLE Controller Layer</td><td colspan="2">Link Layer (LL)</td></tr>
<tr><td colspan="2">Physical Layer(PHY)</td></tr>
</table>

Figure 1: BLE Protocol Structure

The Controller or radio is the lowest block of the BLE protocol and is composed of the Physical Layer (PHY), the Link Layer (LL) and the Host Controller Interface (HCI), serving as the connection between the Controller and the Host. The PHY layer, composed by hardware, uses Gaussian Frequency Shift Keying (GFSK) modulation, Adaptive Frequency Hoping (AFH) for communication between the devices, as well as data packages with the forty-seven bytes of maximum length for sending and receiving data between operations. The Link Layer is the part of the stack that directly interfaces with the PHY, it defines the types of communications that can be created between BLE devices by managing the link state of the radio. LL defines the roles a BLE device can play such as: advertiser, scanner, master, and slave. [3][9]

The Host is composed of various layers such as the Logical Link Control and Adaption Protocol (L2CAP), Security Manager Protocol (SMP), Attribute Protocol (ATT), Generic Attribute Profile (GATT) and the Generic Access Profile (GAP). L2CAP is responsible for handling the data from lower layers to upper layers and vice versa. Data from LL is encapsulated into the standard BLE

packet format according to ATT and SMP. From upper to lower layer, it breaks down or fragments the large data packet into the payload size for sending it via LL and then PHY. The two processes are respectively called recombination (encapsulation) and fragmentation. SMP is responsible for encryption and decryption of data packages, and it defines two main roles during the establishment of a connection: the initiator and the responder. ATT acts to define a client/server relationship, where the client requests data from the server and the server sends data to the client. As well, AAT is responsible for data organization into attributes, assigning a handle, a Universally Unique Identifier (UUID), a set of permissions and a value. The GATT adds a data model and hierarchy, so that the server proposes its services and characteristics to the client to define how data is organized and exchanged between applications. GATT servers or profiles, contains different services that are filled with characteristics. Characteristics contain data value, description, and permission. As an example, a Temperature sensor will have a service, in which the data will be the value of a characteristic. Finally, GAP is responsible for controlling connections and advertising in BLE. Figure 2 presents the structure of a GATT server or profile. [3][9]

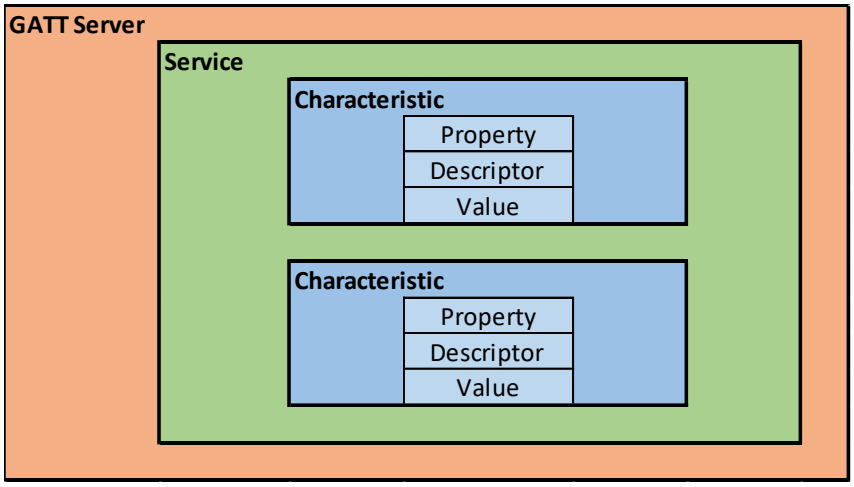

Figure 2: GATT Server Structure

To finalize the BLE background, it is important to understand how BLE devices communicate and function in a network. BLE devices can communicate in two main ways: connections and broadcasting.

On Broadcasting, devices do not establish a connection, advertising packets are sent from a single advertiser to any scanning or receiving device. Even though it is the fastest way to send data to multiple scanners, it is not suitable for sensitive applications because of its lack of security or privacy controls. Broadcasting packets have two main objectives, first to broadcast data to events that do not need connections, and second when a master wants to connect and send advertising packets to slaves available for connection. In depth explanation of the broadcasting properties, such as *scan_interval* will be explained in the Power Analysis sections of this paper. [3][9]

Connection, on the other hand, is continuing private and periodical exchange of packet between two devices. In connections, there are two main players, the Master or Central, and the Peripheral or Slave. The Central looks for advertising devices and initiates a connection. After a connection is established, the master is responsible for managing the settings and starting a periodic packet exchange. The Peripheral periodically broadcast connectable advertising packets and accepts connections initiated by the Central, when a connection is concluded, it follows the commands set by the central [3][9]

2.3. Transmission Line Design

This section explains the three most common Printed Circuit Board design techniques for Transmission Lines which are Microstrip, Stripline, and Coplanar Wave Guide (CPW), and its variation Grounded CPW.

2.3.1. Microstrip

Microstrip features a signal conductor fabricated on top of a dielectric layer, with a ground plane on the bottom of the dielectric material. It features an easy to fabricate structure and is not complicated to model. Overall microstrip is a smart choice for systems within lower bands, however, it suffers from higher radiation losses at higher frequencies, being also susceptible to interference as there is no shielding surrounding the trace. [22-23]

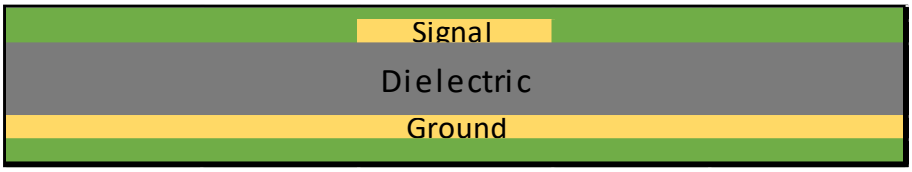

Figure 3: Microstrip Physical Structure

2.3.2. Stripline

Stripline is somewhat similar to a microstrip, as it is a Microstrip with a ground layer above and underneath the dielectric surrounding the conductor, which improves the vulnerability with regards to interference. Nevertheless, Stripline has higher dielectric losses, and as it is in the inner layers of the PCB, getting the signal out of the substrate through vias can cause reflection and interference. [22-23]

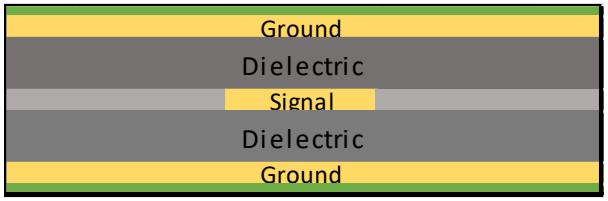

Figure 4: Stripline Physical Structure

2.3.3. Coplanar Waveguide (CPW) and Grounded CPW (GCPW)

In this subsection, CPW and GPCW concepts are examined. CPW has the signal conductor surrounded by ground pours, all on top of a dielectric layer, with an additional ground plane in the bottom. The dimensions of the center strip, the gap, the thickness, and permittivity of the dielectric

substrate determined the effective dielectric constant, characteristic impedance, and the attenuation of the line.

GCPW has the same structure as CPW, with the addition of vias surrounding the conducting trace connecting both the top and bottom ground pours. With vias connecting the ground planes, GCPW is less prone to radiation and has higher isolation than Microstrip limiting the occurrence of signal interference. However, this approach is more difficult to model and manufacture [22-23].

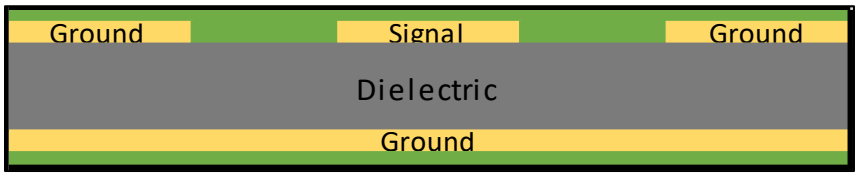

Figure 5: Coplanar Waveguide Structure

2.4. Tools

The work presented in this paper was realized by various tools. This section will give a brief description of the software used for the Printed Circuit Board (PCB) design, Altium Designer, the Integrated Development Environment (IDE) for software development and programming of the main SoC, Code Composer Studio from Texas Instruments (TI), and the Keysight EXR Oscilloscope and Spectrum Analyzer for power analysis, RF measurements and hardware debugging.

Altium Designer is a software package for PCB design and Electronic Design Automation (EDA). It offers schematic capture and design, 3D PCB design, FPGA development and data management. Features such as the different impedances models for transmission lines designs, such as Microstrip and Coplanar Waveguide were important for this project. [13]

Code Composer Studio is an IDE for the development of software for TI-embedded processors. It is primarily designed as for embedded project design and low-level JTAG based debugging, which

is the communication protocol used to program the CC1352 in the custom PCB. It also enabled the integration of the Bluetooth Low Energy stack developed by TI and to the sensors and services designed in this work. No less important, CCS was used for debugging and in the process of hardware bring up, such as verifying crystals status and important registers in the main SoC. [14]

After developing the PCB and properly programming the CC1352 chip, test equipment was used for several evaluations. The EXR208A High Speed Oscilloscope from Keysight, was used for the bring up evaluation of the PCB by monitoring different signals at specific components, for the debugging of serial communication protocols such as I2C and SPI, and finally for the analysis and evaluation of the power consumption of the device at different cycles and operation situations. The E900B Spectrum Analyzer, also from Keysight, was used for the monitoring of the BLE RF signals. It was used first to understand the BLE spectrum, and well as power characteristics. [15]

3. Design

In this chapter, the overall design is described. It starts with the introduction of the main components, followed by the circuit schematic structure, the Printed Circuit Board design process and finalizing with the software development.

3.1. Components

In this section, the main components of the system are introduced, and a brief discussion is presented with the reasons behind each component and its respective use in the final design. The first component to be analyzed is the main SoC, CC1352P7, followed by the three sensors. The chapter is concluded with a block level diagram of the envisioned system.

3.1.1. Texas Instruments CC1352P7

The CC1352P7 SoC is a and multi-band Sub-1 GHz and 2.4GHz wireless microcontroller (MCU) supporting different protocols such as ZigBee, Bluetooth 5.2 Low Energy, IEEE 802.15.4g, proprietary systems, including the TI 15.4-Stack (Sub-1 GHz and 2.4 GHz) and others. It is based on an Arm Cortex M4F main processor and optimized for low-power wireless communication and advanced sensing medical applications, IoT, personal electronics and smart devices.

The CC1352P7 has a software define radio powered by an Arm Cortex M0, allowing support for multiple Physical Layers (PHY) and RF standards, supporting operation in 287 to 351-MHz, 359 to 527-MHz, 861 to 1054-MHz, 1076 to 1315-MHz, and 2360 to 2500-MHz frequency bands. In addition to its main M4F processor, the CC1352 has an autonomous ultra-low power Sensor Controller CPU, which can read and monitor sensors independently of the main processor, therefore significantly reducing power consumption and offloading the main CPU. It supports different MCU peripherals, such as SSI, I2C, UART while also having a 12-bit ADC for analog sensors.

The SoC has a low sleep current of 0.9 μA, an MCU consumption of 2.63 mA on active mode, and an ultra-low consumption of 25.2 μA when using only the sensor controller CPU at 2 MHz and 0.7 mA when at 24 MHz mode. With respect to the radio, it is 6.4 mA for RX and 21mA for TX at 2.4GHz.

With such characteristics and specifications, the CC1352P7 MCU is ideal for the constraints of the design of a lowpower multi-sensor device. Its dual-band capabilities can be key for the exploration of applications outside of the BLE scope, specifically with the long-range use of the Sub-1 GHz radio. In addition, its low-power consumption, Serial Peripheral support, and the 12-Bit ADC enables it as a strong platform for low-power multisensory applications which is the focus of this work

3.1.2. Sensors

With the objective to design a multisensory platform to reach the maximum number of applications, but also with size constraints, it was decided that three sensors, enabling a total of 6 different measurements would provide desirable scalability for the final sensor node.

BME688

The BME688 is a 4 in 1 sensor capable of measuring pressure, temperature, humidity, and gas. It has a compact package and is especially developed for mobile & connected applications where size and low-power consumption are critical requirements. The gas sensor through the integrated Artificial Intelligence (AI) can detect Volatile Organic Compounds (VOCs), volatile sulfur compounds (VSCs) and other gases such as carbon monoxide and hydrogen in the part per billion range. It fits extremely well with the purpose of this paper as it is adaptable to multiple applications and provides solid energy efficiency.[16]

ADXL343BCZ

The ADXL343 is a versatile 3-axis, digital-output, low *g* MEMS accelerometer, suitable for sensing acceleration in various applications. ADXL343 can measure the static acceleration of gravity in tilt-sensing applications, as well as dynamic acceleration resulting from motion or shock, its high resolution enables measurements of inclination deviations for less the one degree. The sensor supports the BME688 in different applications and measurements, extending the reach of the multisensory platform.[17]

AD5941

The last sensor of the design is the AD5941, a high precision, low-power analog front-end (AFE) designed for portable applications requiring impedance measurements, such as those from skin and body. Such characteristics complete the overall scalability of the platform, leveraging a device with small footprint to many uses.[18]

3.1.3. Hardware Diagram

The block diagram in Figure 6, represents the overall structure of the system. It is important to highlight the power source chosen of a 1025-coin cell battery to fit with size constraints.

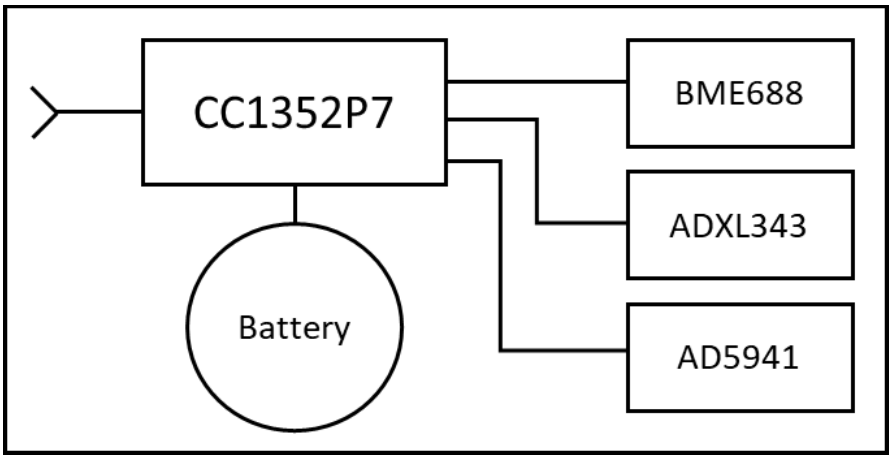

Figure 6: YSU SensorTag Hardware System Diagram

3.2. Schematic Design

The schematic of the multi-sensor node is designed around the characteristics of the CC13X2 series of SoCs by Texas Instruments and most of it is part of TI recommended schematic. Therefore, in case a chip replacement is needed, the same circuit can be used. The schematic is also designed so that future modifications are only performed when sensors need to be added or exchanged depending on the application, leaving the analog and RF sections with the original design. However, modifications can be made depending on the final purpose of the system and its objectives.

In this section, the circuit schematic design is presented and explained. The main characteristics covered are crystal oscillators required by the main SoC, the RF front-end, sensors communication, as well as the power circuit.

Starting with the clock system, the main SoC has several internal clocks. A 48 MHz is used as the main MCU and peripherals clock. It can be driven by the internal 48 MHz oscillator or an external 48 MHz crystal oscillator. However, the Radio operation requires an external 48MHz, which is connected to the MCU. A lower frequency clock of 32.278 kHz is also present in the schematic serving for applications such as the Sensor Controller Studio and where the main MCU requires a very precise and refined frequency.

Moving forward with the schematic, the 3 sensors were connected to the MCU via Serial Peripheral Interface, utilizing a total of six pins. The sensors share a common clock wire, defined by SCK, and the two data channels defined by MISO and MOSI with the CC1352. Lately, each sensor has its own Chip Select pin defined by CS. A block diagram for the SPI connection is in Figure 7.

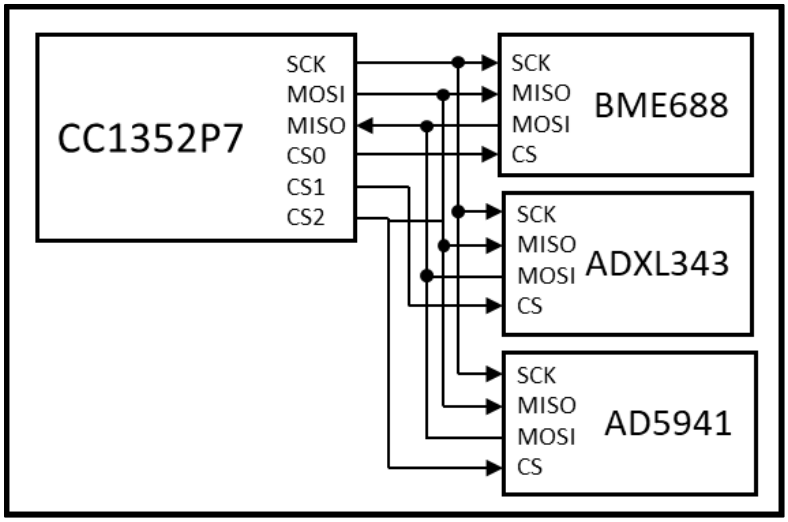

Figure 7: SPI Connection Diagram

For the RF front end, there are two set ups, Differential and Single-ended, together with an external or internal bias. In the design the RF front-end is a combination of Single-ended and external bias. The decision for the set-up was made as tradeoff between a theoretical -3dB loss in output power when compared to the Differential front end, but with a desirable economy in components that would make the final PCB smaller and with a low cost, as the main objective of the design was to be compact, cost and energy efficient.

The CC1352 has three power rails that are exposed on external pins: VDDS, VDDR and DCOUPL. VDDS is the main power source for the wireless microcontroller and must be supplied externally with 1.8 V to 3.8 V, therefore decoupling capacitors are placed on each pin to avoid potential difference fluctuations. VDDR is an internal power rail that is supplied from the internal DC/DC converter, or the internal Global LDO, but can be powered from an external supply. To perform such modification, a capacitor is removed from the schematic, leaving an open circuit between the DCDC converter and VDDR. VDDR is regulated to approximately 1.68 V, or 1.95 V when running in boost mode for maximum output power in sub-1 GHz bands. DCOUPL is supplied internally

by either Digital LDO or Micro LDO depending on the power state. This power rail is trimmed to approximately 1.28 V and requires an external decoupling capacitor of 1 µF.[19]

3.3. Printed Circuit Board Design

With the intent to create a compact and efficient multi-sensor platform, the development of a custom Printed Circuit Board makes the system available for various applications as a ready to use device. This section explains the design process of the PCB, starting from the overall concept and shape, following by and explanation of important aspects of the layer stack, impedance matching for the antenna transmission line, the coin cell battery, and other peculiarities of the TI SoC.

3.3.1. Overall Concept and Shape

The PCB is designed to be a low cost, compact and efficient, with the capability of being implemented in various applications, many times serving as a disposable sensor node, as an example when measuring elevated temperatures of sand casting. The final PCB is of rectangular shape with a size of 29.75 by 36.5 mm and thickness of 1.6 mm. When serving as a disposable sensor node, the programmable interface of the PCB can be detached once programmed, reducing the final implantable size by 25% to 29.75 by 27.25 mm. Figure 8 presents the PCB layout.

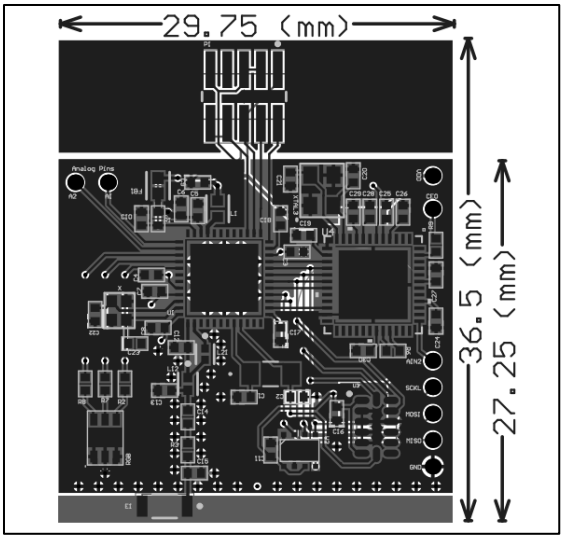

Figure 8: PCB Layout and Dimensions

3.3.2. PCB Layer Stack

RF designs at the ISM band of 2.4 GHz can be complex, most of the time involving Analog, Digital and RF signals. Therefore, a few considerations must be analyzed before deciding how many layers the PCB should have. Such considerations will range from the number of connections, return path for RF signals, impedance matching calculations, cost, as a board with more layer's result in higher cost and others. In this case, it was decided to pursue a 4-layer board stack up. In an RF design, great isolation between signal layers is very important to avoid cross talking and signal interference, therefore, the stack up was separated in the disposition indicated in Figure 9. Where the Top and Bottom layers are responsible for Signals and Power, and Layer 2 and Layer 3 are the ground planes. By choosing this stack, the RF signals in the top layer are shielded from the signals and power lines of the bottom layer, avoiding any major interference. The thickness of each layer is determined first by the total thickness of the board, and the different copper thickness offered by the manufacturer. The dimensions are also a crucial factor for the calculation of the microstrip impedance, which is covered in the next section.

Name	Type	Thickness(mm)
Top Solder	Solder Mask	0.01
Top Layer	Signal + Power	0.035
Dielectric	Prepreg	0.175
Layer 2	Ground	0.035
Dielectric	Core	1.1
Layer 3	Ground	0.035
Dielectric	Prepreg	0.175
Bottom Layer	Signal + Power	0.035
Bottom Solder	Solder Mask	0.01

Figure 9: PCB Layer Stack

3.3.3. RF Transmission Line Design and Impedance Matching

The transmission line from the SoC to the antenna is certainly one of the most important parts of the PCB design process. Proper impedance matching is crucial for the signal propagation and low reflection, and trace shielding through copper planes and vias isolates the RF signal from potential interferences, allowing a clear path from the chip until the antenna.

In this section, the RF transmission line design is explained, providing how the technique chosen is appropriate for this design, as well as the calculation for the width of the trace to match the impedance and the PCB layer structure.

Usually, transmission lines to an antenna have a 50 Ohm impedance, therefore the trace is modelled so that it matches the desired specification. To provide proper matching, certain considerations must be made, primarily the type of trace to be implemented. The three most common approaches are Microstrip, Stripline, and Coplanar Waveguide (CPW) which has a variation as of Grounded CPW (GCPW) as described in the literature review section 2.3.

For this design it was decided that GCPW would be used, as it presents superior isolation and lower loss when compared to the other techniques. The structure of GCPW is displayed in Figure 10.

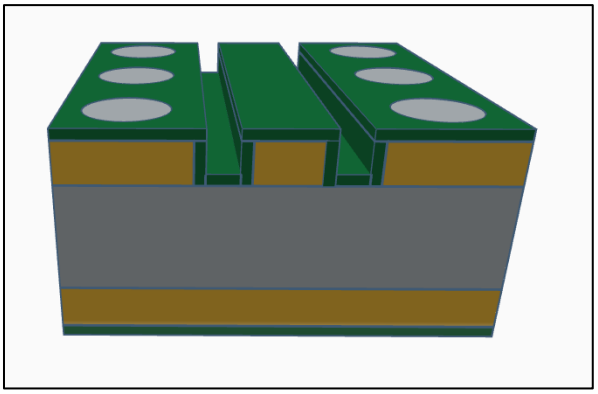

Figure 10: Actual PCB Grounded Coplanar Waveguide Structure

The first step after selecting GCPW is to calculate the dimensions of the trace so that the conductor is at a 50 Ohms impedance. This calculation was performed on Altium Designer, achieving a final width of 0.2388 mm, and can also be found by using the set of Equations from 1.1 to 1.6. [20]

$$Z_0 = \frac{60.0\pi}{\sqrt{\varepsilon_{eff}}} \frac{1.00}{\frac{K(k)}{K(k')}+\frac{K(k1)}{K(k1')}} \qquad \text{Equation 1.1}$$

$$k = \frac{w}{s} \qquad \text{Equation 1.2}$$

$$k' = \sqrt{1.0 - k^2} \qquad \text{Equation 1.3}$$

$$k1' = \sqrt{1.0 - k1^2} \qquad \text{Equation 1.4}$$

$$k1 = \frac{\tanh\left(\frac{\pi w}{4.0h}\right)}{\tanh\left(\frac{\pi s}{4.0h}\right)} \qquad \text{Equation 1.5}$$

$$\varepsilon_{eff} = \frac{1.0+ \varepsilon_r \frac{K(k')\,K(k1)}{K(k)\,K(k1')}}{1.0+ \frac{K(k')\,K(k1)}{K(k)\,K(k1')}} \qquad \text{Equation 1.6}$$

Following the width modeling, the next step is to Layout the trace in the PCB. In such process, the components that are part of the transmission line are placed so the trace would have a straight path. In case of any angled connections, they should be performed preferably at 45 degrees angles and avoiding sharp edges. There should not be any connections crossing the RF transmission line in lower layers. In conclusion, as part of the GCPW design, vias are placed adjacent to the traces forming a shield, and a ground conductor is poured around the transmission line concluding the GCPW design. This process is shown in Figure 11, where the red plane is the ground pour. [19][21]

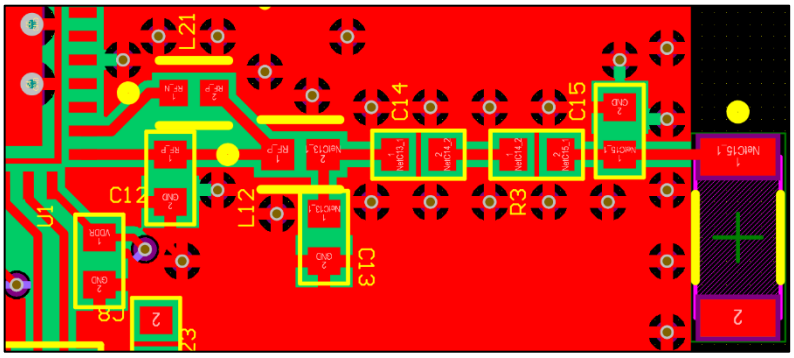

Figure 11: RF Transmission Line Grounded Coplanar Waveguide (GCPW) Design

3.3.4. Crystals and Decoupling Capacitors placement

Apart from the Transmission Line design, important components such as the Crystal oscillators and decoupling capacitors must be placed accordingly in the PCB layout.

For crystals, as the main oscillation loop current is flowing between the crystal and the load capacitors, the signal path from capacitor to crystal should be as short as possible using a symmetrical layout, and both capacitor ground connections should also be as close as possible. Finally, ground routes should never be routed around the crystal, as the trace is susceptible to cross talking and electromagnetic interference.

Regarding the decoupling capacitors, they should be placed near the power pins of the SoC and should have a separate trace or via to ground to minimize noise coupling. [19]

3.4. Software Implementation

This section is intended to briefly explain the software implementation Bluetooth Low Energy (BLE) and the setup of the SPI interface between the SoC and sensors.

As previously mentioned in section 3.2, the sensors present in the design are connected to the main chip via Serial Peripheral Interface (SPI). With SPI, the sensors share the core communication lines of clock, represented by SCK, and data in and out terminals defined by MISO and MOSI, later the Chip Select (CS) line is connected to each sensor in other to start and operation.

To start an SPI transaction, first the SPI module is initialized, enabling distinct functions and handles to be called. Later when the sensor is turned on via Bluetooth, several steps are performed until the data is read from the sensor enabled.

First, the SPI parameters are defined, such as frame format, bit rate, and data size. Later, the SPI bus is opened, to initialize a connection between the Master, the CC1352, and the slaves, the sensors. Upon opening the SPI bus, the data collection is ready to be performed, the Chip Select for the responsible sensor is turned active, depending on the sensor, it is configured to LOW or HIGH, establishing a closed communication between the host and that specific sensor only, so that read and write transactions can be performed.

Furthermore, the data buffers for reading and writing are defined and the number of transactions to be performed. The MOSI starts the interaction by writing a 7-bit address to the sensor and an 8^{th}-bit signaling a READ, set to 1, or 0 to WRITE, operation. In case the transaction is written to the slave, the bus following the address has the data, and the MISO line, responsible for data coming from the sensor is disregarded. In a READ operation, after the address is written with the eighth bit set HIGH, the MISO line is then responsible for streaming the data from the slave to the

master. At the end of the operation, the CS line is returned to its original state, closing the direct communication between the Master and Slave.

On Figure 12, a part of the SPI driver code for the ADXL383 sensor presents the process described above, starting on the initialization of the SPI parameters, then opening the SPI bus, setting the RX and TX data buffers, transaction count, following by performing the data transfer with the SPI_transfer command, and finalizing by restoring the CS to its default value.

```
/* Open SPI as master (default) */
SPI_Params_init(&spiParams);
spiParams.frameFormat = SPI_POL1_PHA1;    // Polarity 1 (idle state) Phase 1 for ADXL343
spiParams.bitRate     = 100000;           // 100KHz
spiParams.dataSize = 8;                   // 8-bit data size
spi = SPI_open(CONFIG_SPI_0, &spiParams);

/* Transaction to Get Sensor ID */
GPIO_write(ADXL343_CS, 0);
txBuffer[0] =  0x00 | ADXL343_READ;
spiTransaction.count = 2;
spiTransaction.txBuf = (void *)txBuffer;
spiTransaction.rxBuf = (void *)rxBuffer;
transferOK = SPI_transfer(spi, &spiTransaction);
GPIO_write(ADXL343_CS, 1);
```

Figure 12: SPI Initialization and Read Transaction in ADXL343 Sensor

Figure 13 presents a Digital Waveform from an SPI transaction captured in an Oscilloscope. It is that the transaction starts when the CS line, indicated by channel D7 is turned LOW and stops when CS is HIGH. Channel D4, represents the CLK line, which operates based on the CS line time. Also, it is possible to identify Write operations, when the MISO line, represented by channel D6 is static until, and a Read operation is when the MOSI line, on waveform channel D5 is always LOW when no data is flowing.

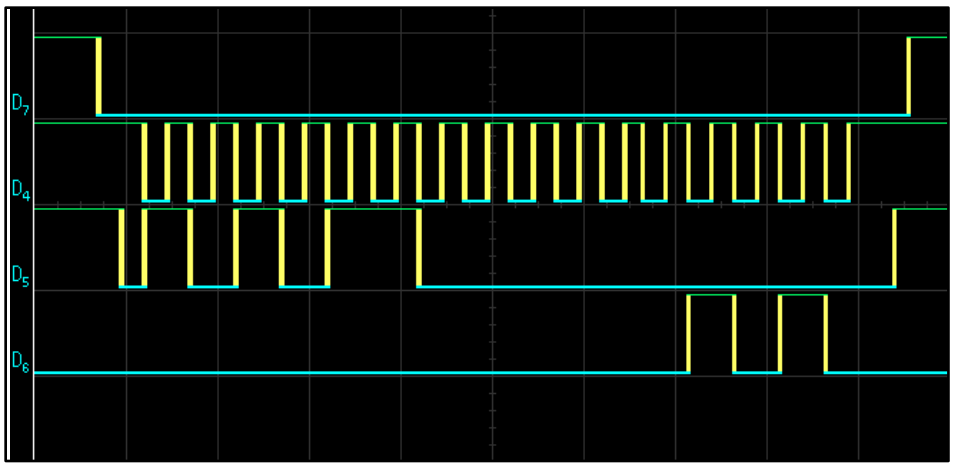

Figure 13: SPI Transaction Waveform

3.4.1. BLE Implementation

This section presents the structure of the BLE Peripheral for the design being presented, and the following subsections explain the Texas Instruments BLE Stack and the interface between BLE and the Sensors.

To establish a steady communication between a smart device and the platform developed, with control and data flow from both devices, key parameters were defined. First, the sensor node is set up as a peripheral device, while the phone or computer serves as the central. In sequence, it was defined that each sensor would have its own service, comprised of 3 characteristics, with distinct properties and functionalities:

- Data Characteristic: serving as the characteristic responsible to read sensor data, has the GATT Read and Notify properties.
- Config Characteristic: responsible for configuring the sensor, which means turning it On or OFF, has the GATT Read and Write properties.
- Period Characteristic: responsible for setting up sensor sampling rate, has the GATT Read and Write properties.

An LED service, with GATT Read and Write properties, serving for debug and process indication, complements the BLE peripheral structure of the device, presented in Figure 14.

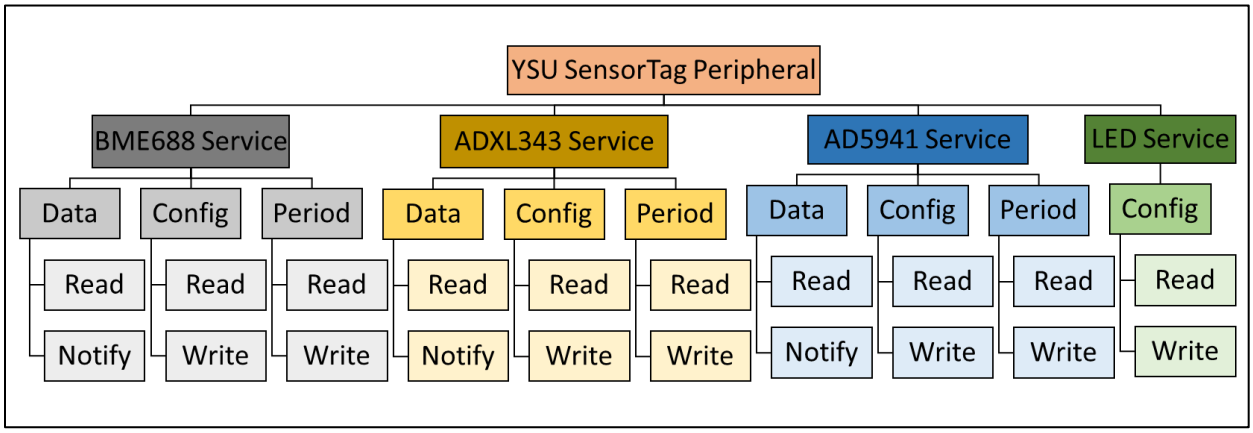

Figure 14: BLE Peripheral Structure of YSU Sensor Network

3.4.2. BLE and Sensors Interface

The interface between the BLE and Sensors can be complex, as there are specific functions to be performed by the BLE Stack for each part or event of the process.

A service, is comprised of the many attributes, as explained in Section 2.2, in a software perspective, a service has 4 main functions used when the device is in operation, which are:

1. `AddService()` function: Initializes the corresponding service by registering GATT attributes with the GATT server.
2. `RegisterAppCBs ()` function - Registers the application callback function.
3. `SetParameter()` function - Set a corresponding service parameter, in synthesis, from the SoC back to the smart device.
4. `GetParameter()` function - Get a corresponding service parameter, in synthesis, from the SoC back to the smart device.

The Peripheral profile, in a software level, has numerous functions, which varies from linking the application layer the physical layer, as explained in section 2.2, as well as calling application-level functions of the services, serving as an organizer between all sensors. However, for this case, three functions are particularly important and introduced for better understanding of the interface between BLE and sensors.

1. `charValueChangeCB()` function - indicates a characteristic value change in the services, identified by the sensor callback.
2. `processAppMsg()` function - process an incoming callback from a profile.
3. `processCharValueChangeEvt()` function - process a pending profile characteristic value change event, called by the `processAppMsg()` function.

Last, an important local function from each sensor, which is:

5. `processCharChangeEvt()` function – called by the `processCharValueChangeEvt()`, when a configuration or period values has changed.

With that, it is possible to explain the overall cycle of the integration between the Sensors and the Bluetooth Low Energy, which is presented in Figure 15.

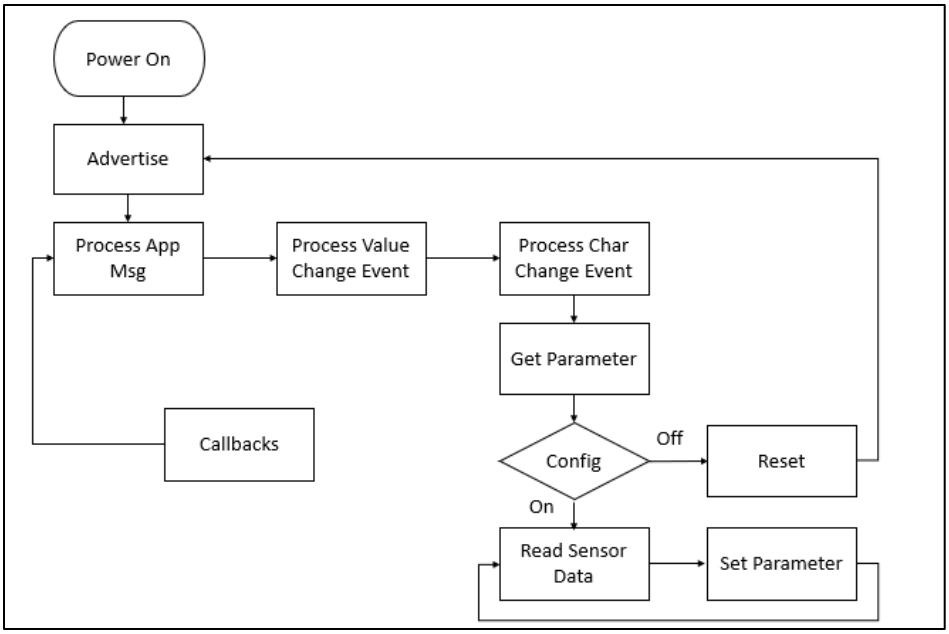

Figure 15: BLE and Sensor Integration Cycle

Upon starting the peripheral device and connecting it to a central, connection is established, the Services are initialized by the **`AddService()`** function of each sensor. Later, when going into the Config service of the respective sensor, and writing 1 to the Config Value characteristic, the **`processAppMsg()`** on will be called, and as an event characteristic has changed, it will call the **`processCharValueChangeEvt()`** function, so it processes which characteristic the event has occurred as UUID of the characteristic is passed as identification, by calling the **`processCharChangeEvt()`** of the sensor. This process is shown in Figure 16, with the `processCharValueChangeEvt()` function code.

```
static void YSU_processCharValueChangeEvt(uint8_t paramId)
{
  uint8_t newValue;

  switch(paramId)
  {
    case ADXL343SERVICE_ADXL343CONFIG_ID:
        ADXL343_processCharChangeEvt(paramId);
      break;

    case ADXL343SERVICE_ADXL343PERIOD_ID:
        ADXL343_processCharChangeEvt(paramId);
      break;

    case BME688SERVICE_BME_CONFIG_ID:
        BME688_processCharChangeEvt(paramId);
      break;

    case BME688SERVICE_BME_PERIOD_ID:
        BME688_processCharChangeEvt(paramId);
    break;

    case RGBLEDSERVICE_RGBLEDCONFIG_ID:
        RGB_processCharChangeEvt(paramId);
    break;

    default:
      // should not reach here!
      break;
  }
}
```

Figure 16: Function to Process Characteristic Event Change

Later, the **`GetParameter()`** is called, and the value written to config is then stored. The sensor is turned on, processes the data, which is then passed to the **`SetParameter()`** function to be updated in the app. The **`SetParameter()`** process is repeated for each time new data is collected.

The overall process is performed for each specific characteristic change, and its respective nested functionalities.

4. Test Methodology

To evaluate the sensor node developed in this work, two main categories of the design are analyzed. First, with respect to the Radio Frequency (RF) performance, and second the power consumption of the device at distinct stages of the BLE connection and sensor operation cycles.

The RF tests, performed in the Keysight Spectrum Analyzer N9000B and the Vector Software Analysis for digital demodulation, aim to verify the Bluetooth characteristics and power output of the device. Initially, the overall spectrum of BLE is captured at the advertising frequencies, where the output power is analyzed. The RF test is finalized with a sensitivity test. Receiver sensitivity measures the minimum signal strength a receiver can interpret, which means the lowest power level at which the receiver can detect a radio signal, maintain a connection, and still demodulate data. Bluetooth technology specifies that a radio device must be able to achieve a minimum sensitivity of -70 dBm, with such parameter being defined when a Bit Error Rate of 10^{-3} is reached. [22], [23]. Finally, the device Receiver Signal Strength Indicator (RSSI), which is another measurement of power level at the receiver is gathered and compared to existing design with a differential front end.

Such tests enable a comparison between the Single-Ended antenna sensor node to a differential front-ended device from TI. This correlation has the intent to demonstrate the tradeoffs between using each method and how each design is impacted by its front-end characteristics.

The setup of the spectrum analyzer is displayed in Figure 17. A 2.4 GHz Whip Antenna serves as the RF input, and captures the signals in the environment, and the custom PCB is placed as close as possible to the antenna. Later, the VSA software is setup, and a new measurement is created using the Bluetooth demodulation. The frequency is set to 2.402 GHz, so it captures advertising

channel 26, and a trigger is placed at 1.1 mV, to so that the Spectrum Analyzer only records the BLE signals with a threshold in strength.

Figure 17: RF Evaluation Test Set Up

Second, the sensor node is evaluated with regards to its power consumption at various stages and cycles of operation. The device is evaluated at different events, such as when in Advertising and Scan modes, as well as with different parameters that are crucial for overall power analysis such as scan interval, advertising interval and transmission output power. During advertising, through the current draw, it is possible to observe the eight distinct stages of the cycle which are individually explained.

Sequentially, the device is evaluated with the sensors On and Off, analyzing the overall consumption to predict a battery lifetime as well as how the behavior of sensor operation and data transmission takes place. All the tests are performed in the Keysight Oscilloscope EXR 208A. To conclude, the overall consumption of the sensor node is compared to other designs from the research community.

In order to smooth the data from the Oscilloscope and reduce the noise variation, the datapoints manipulated on MATLAB with a running average of 100 to 300 datapoints depending on the size of the final graph. This way, BLE events such as channel transitions, SoC wake-up and others are easier to identify.

5. Results

In this chapter, the results from the tests described at the Test Methodology in Chapter 4 are presented. Section 5.1 lays out the RF tests, performed in the Spectrum Analyzer, whether section 5.2 is responsible for the Power Consumption evaluation. Figure 17 highlights the finalized design and the board realization of the YSU SensorTag comprising of the TI CC1352, and three sensors.

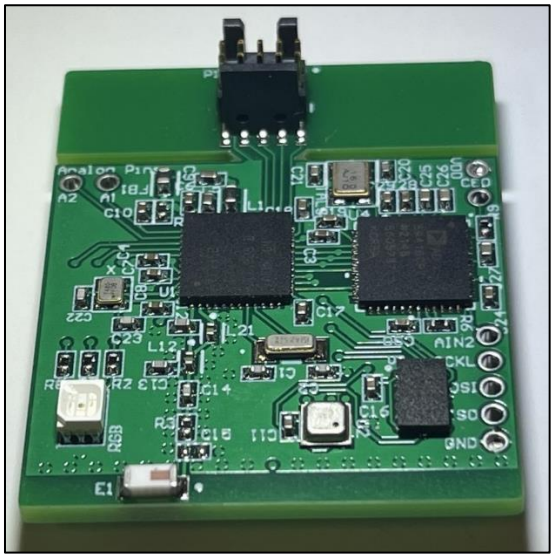

Figure 18: YSU SensorTag - Device Realization Printed Circuit Board

5.1. RF Evaluation

In the RF performance evaluation, the custom PCB is acting as a peripheral device with transmission power set to 5 dBm, in advertising mode, with the set up described in section 4. Figure 19 and 20, present the Spectrum on the Bluetooth Low Energy signal, where in 19 the bandwidth is 10 MHz, capturing a broader view of the signal, and 20, a narrower and in-depth view of the signal over 4 MHz. The peak power of the signal is – 46.5 dBm, considered to be a strong signal performance for the Single-Ended design when compared to the Differential and original design of commercially available devices from TI. The sensitivity of the system is also measured. [22], [23]

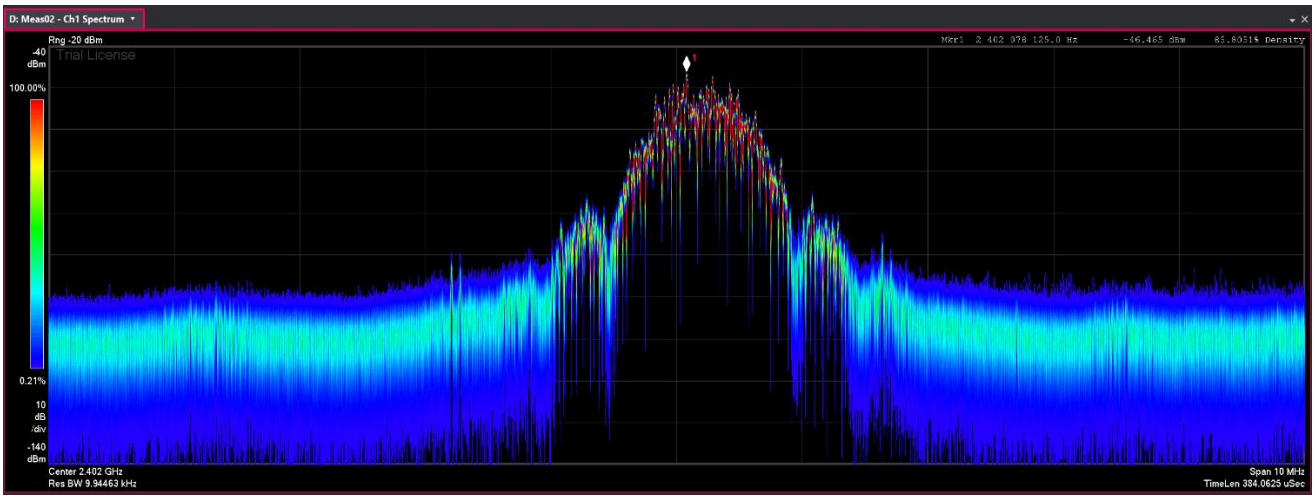

Figure 19: BLE RF Signal 2.402 GHz, span of 10 MHz

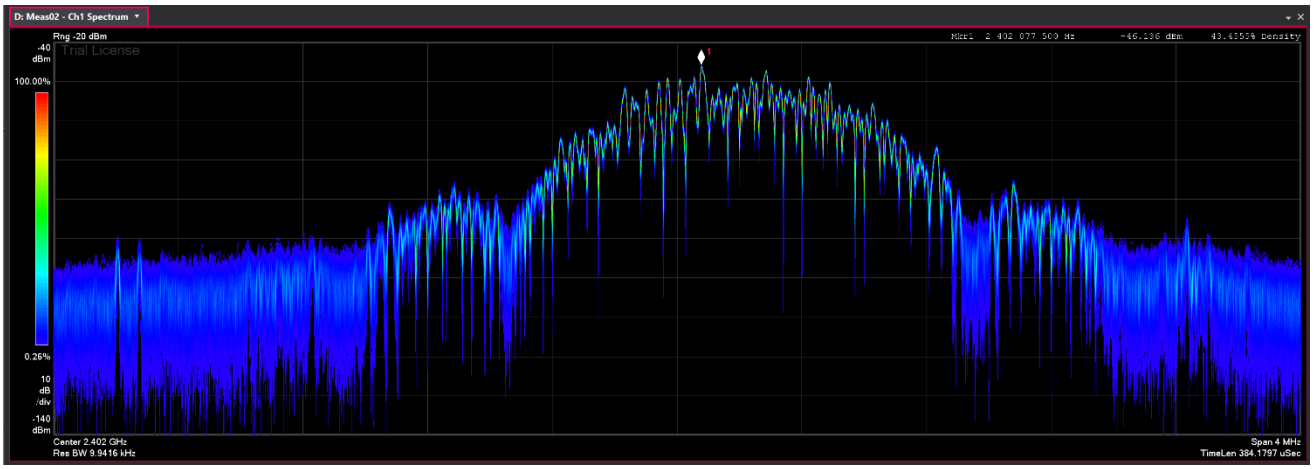

Figure 20: BLE RF Signal 2.402 GHz, span of 4 MHz

On Figure 21, the Power vs Time it is possible to analyze for how long the BLE is advertising based on the Power level and if there are any power variations or drops during the event. The plot shows steady power, at around -46 dBm throughout the whole transaction, only dropping after the advertising event is over, demonstrating once more the desired behavior of the peripheral device.

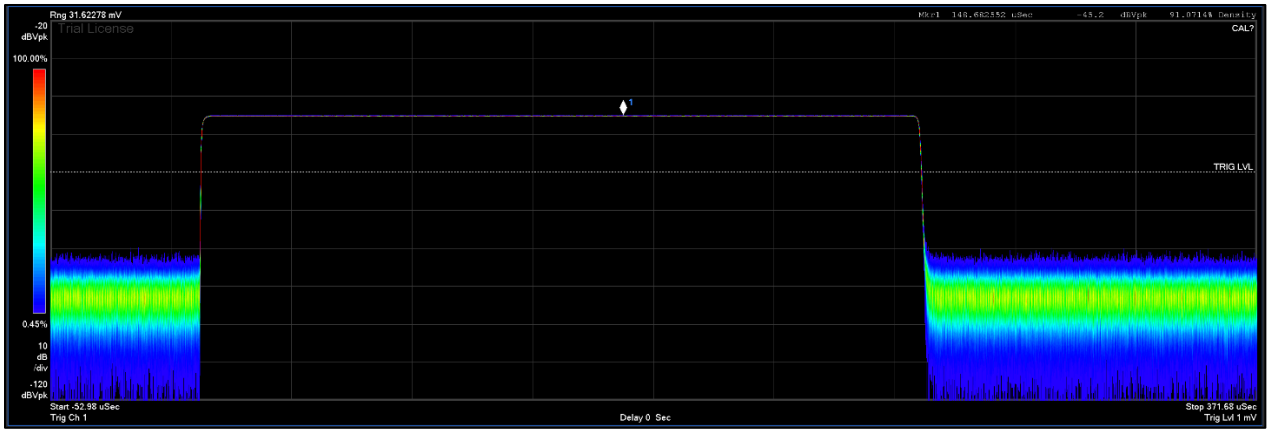

Figure 21: BLE RF Evaluation, Power vs Time

The RF evaluation is finalized by calculating the receiver sensitivity and by measuring the RSSI, with a 2 meters distance, which is the same used by TI for the evaluation of a differential front-end device. The achieved RSSI of the sensor node was -80 dBm, which is better than the -90dBm from the reference design from TI, showing a strong performance from single-ended front-end design. The BLE device achieved the desired Bit Error Rate larger then 10^{-3} when the RX power was at -92.6 dBm.

5.2. Current Consumption Analysis

5.2.1. Advertising state

The first test performed with the sensor node has the intent to monitor the current consumption of an Advertising event. In such an event, the Peripheral and Central devices have not yet established a closed connection, and the advertising data is broadcasted in the Advertising channels 37, 38 and 39, in sequence. By monitoring the current consumption, it is possible to capture all the states of a BLE advertising event sequentially, and assure the device is operating as expected. For this test, the TX power is set to 5 dB, and the *advertising_interval* to 100 ms, which means, every 100 ms one advertising event will happen. If this interval is increased, less power is consumed as the SoC

will be in sleep mode for longer time. Figure 22 shows a full advertising cycle with each number corresponding to a specific stage of the full cycle, from SoC Wake-Up, Channel Hoping and to back to sleep mode.

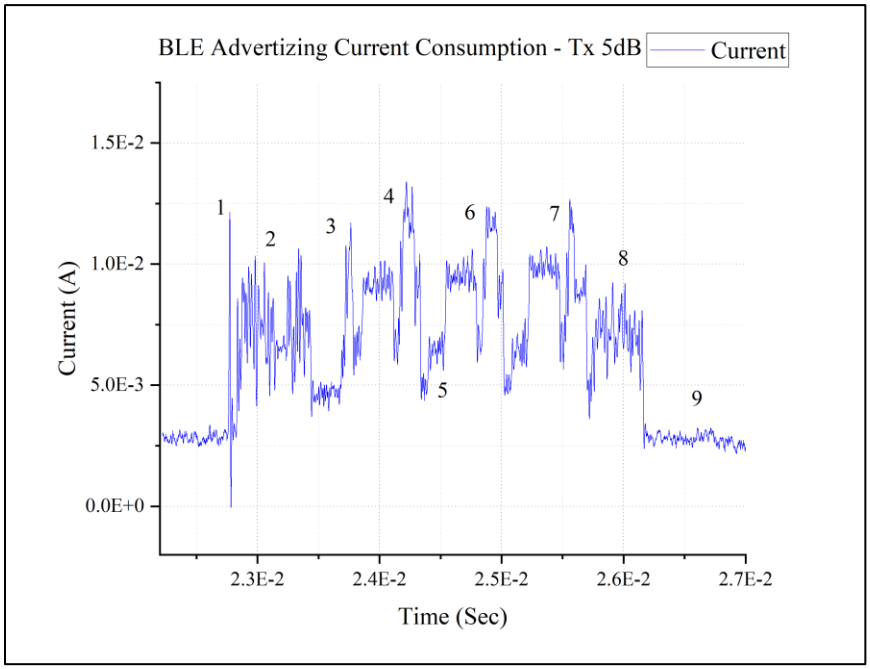

Figure 22: Advertising Event of a BLE Device

1- SoC Wake Up: Starting from the spike of the voltage regulator wake up followed by MCU wake-up.
2- Pre-processing: current increases slightly and the BLE stack prepares the radio for receiving and sending data.
3- Pre RX/TX: Current increases to the level need for pre-Rx state and the BLE radio turns on in preparation of Rx and Tx.
4- Advertising on channel 37: Current increases as BLE radio receiver listens for a packet from the Master on Channel 37, at 2.402 GHz, then current drops as the BLE receiver

stops, and the radio prepares to transmit a packet, finishing the cycle with another increase as BLE radio transmits data to the master.

5- Frequency Hopping and Channel change: Current decreases as the first event is finalized, and prepares for the process of changing the advertising channel.
6- Advertising on Channel 38: hopping characteristic switches to Advertising channel 38, at 2.426 GHz, performs same process as explained in step 4.
7- Advertising on Channel 39: the frequency switches to Advertising channel 39, at 2.480 GHz, following the steps described in 5, perform the same process explained in step 4.
8- Current drops to the level needed for the post processing state as the BLE protocol stack processes the received packet and sets up the sleep timer in preparation for the next connection event.
9- Current drops slightly as the BLE protocol stack prepares to go into sleep mode.[9]

To conclude, the average current draw during the Advertising event was 6.2mA through 5 milliseconds, resulting in a very low-power device.

5.2.2. Scanning State

In a Scanning Cycle, the Peripheral and Central device have established a secure and closed connection, in this state the Peripheral waits for commands from the Central to perform an action. The SoC goes through the same process of Wake-Up, pre-processing, and Pre RX/TX as described in Section 5.2.1, but does not hop between channels, therefore, being a lower time and consumption cycle. The Scanning event is illustrated in Figure 23 and has a final average current draw of 4.1 mA through 2.5 milliseconds. The *scanning_interval* is set to 100 ms, which means, that the device will scan for 100 ms before going into sleep mode again. If this interval is increased, less power is consumed as the SoC will be in sleep mode for longer time.

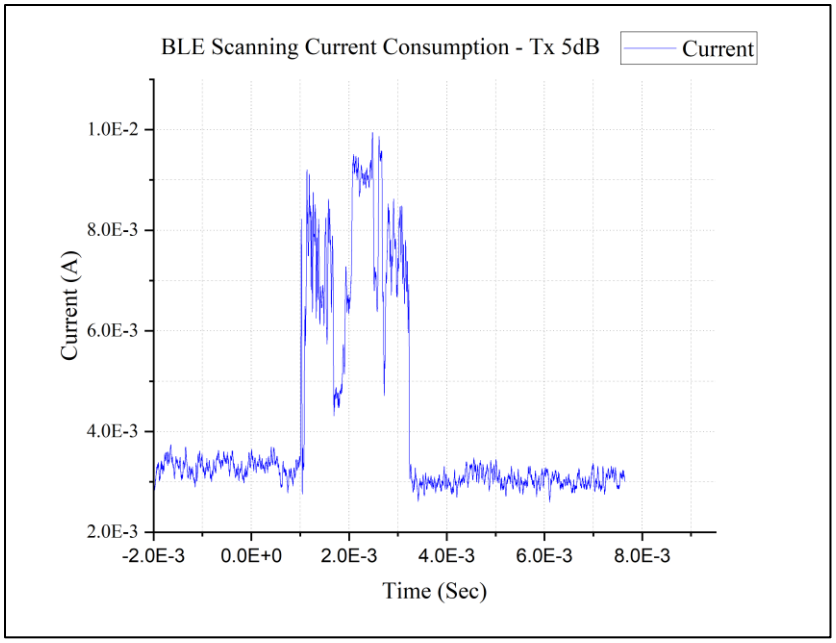

Figure 23: BLE Scanning Event

5.2.3. ADXL343 Operation and Data Transmission

Upon testing the sensor node in Advertising and Scanning setups, an evaluation of the accelerometer ADXL343 was performed. This analysis is intended to not only test for the overall consumption of the sensing cycle, but also to compare and identify the BLE data transmission current draw to from the operational phase. The sensing cycle is represented in Figure 24, starting as well with the SoC wake, indicated by number 1, followed by the sensing period and data read from the ADXL343, indicated by 2, and concluding with the BLE transaction slightly increase in current consumption as identified by.

The final average consumption for sensing and transmitting the data of the Accelerometer is 4.1 mA, this number encapsulates not only the sensor power requirements for operation, but also the transmission of 6 bytes of data, highlighting that a longer Transmission packet will mean more power used during BLE transmission.

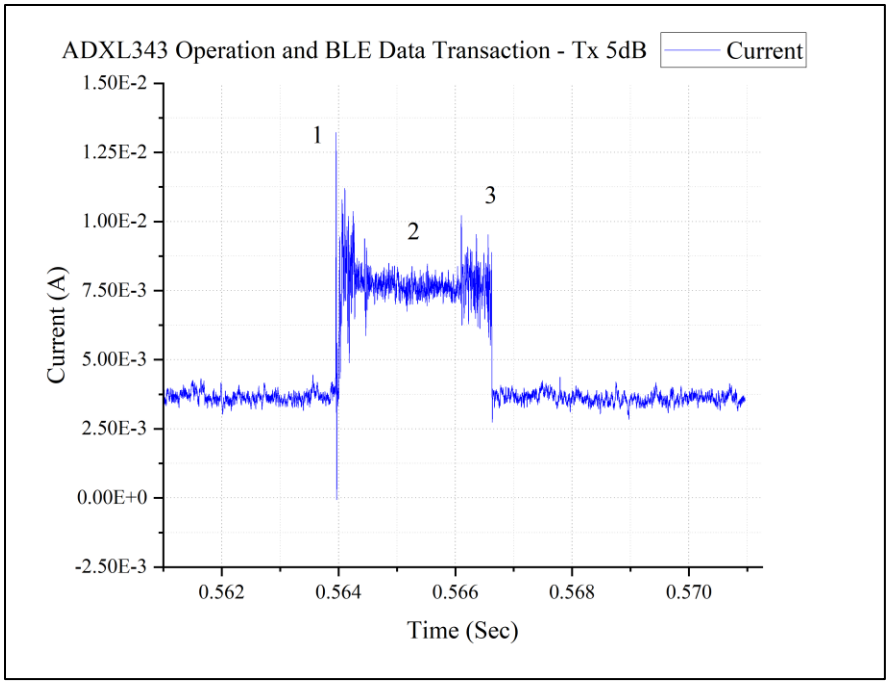

Figure 24: ADXL343 Operation and BLE Transaction Current Consumption

5.2.4. BME688 Operation and Data Transmission

The evaluation of the BME688 sensor was performed in the same manner as the ADXL343 as explained in section 5.2.3, and it is presented on Figure 25. The sensor is set to force mode, which means it performs one measurement cycle and then goes back to sleep mode. The sensing events are in sequence numbered from 1 to 5. On 1, the SoC wakes up and connects to the device, on 2 it performs the SPI transactions for sensor set-up as well as the measurements from Temperature, Humidity and Pressure. On 3, the process for gas resistance measurement is started with a spike in the current levels as the sensor hot plate heater is initialized, later, on 4, the hot plate heated to 300 degrees Celsius over the course of 100 milliseconds, which is seen in a constant increase in current on Figure 25. After that, on 5 the Gas resistance data is acquired, and the overall data is transmitted via BLE. Finalizing the whole measurement and transmission of the Temperature, Humidity, Pressure and Gas Resistance data. The total length of the transmitted packet is 14 bytes, which

also makes the transmission event longer eventually consuming more power than the ADXL343 sensor. As the sensing cycle for the BME688 is extensive and has a high consumption for the gas measurement, the final averaged current draw during the whole operation was of 7.1 mA.

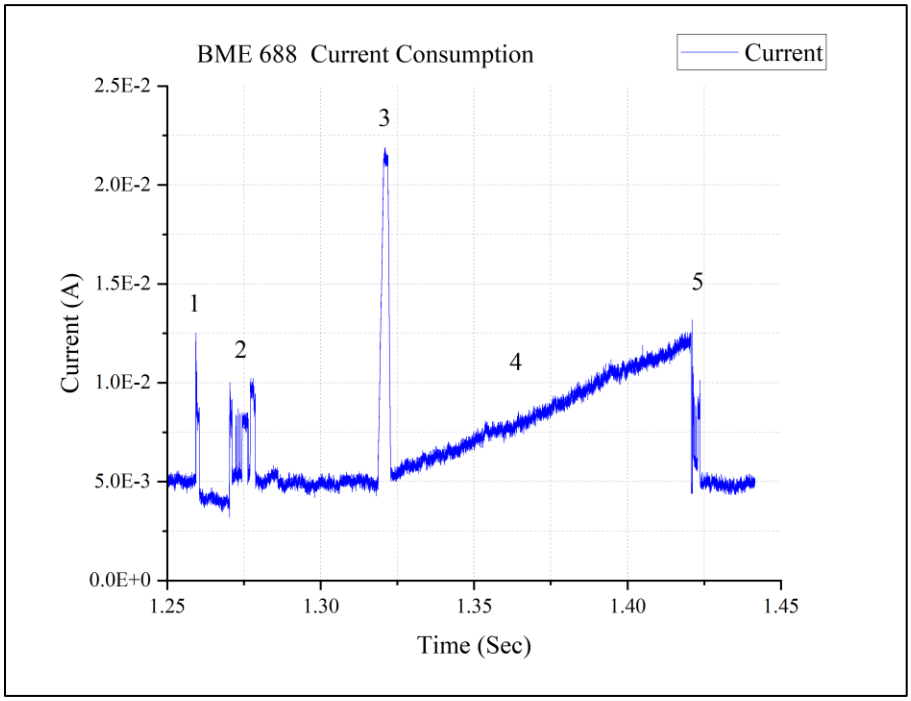

Figure 25: BME688 Operation and BLE Transaction Current Consumption

5.2.5. Device Comparison

This section presents a table with compiled results from BLE devices developed in various research with the minimum of one sensor in operation. The rows in yellow in the table of Figure 26, represent the work developed in this thesis.

Application/Sensor	SoC	SoC Manufacturer	Current (mA)	Reference
Multiple/ ADXL343	CC1352P74	Texas Instruments	4.1	-
Multiple/ BME688	CC1352P74	Texas Instruments	7.1	-
Animal Monitoring	BLEISP150AX	Nordic Semi	3 to 9	[4]
Agriculture IoT	CC2541	Texas Instruments	13.5	[5]
Animal Monitoring	CC2650	Texas Instruments	6	[24]
Health Monitoring	nRF24L01	Nordic Semi	7	[25]

Figure 26: Devices Comparison in terms of Current Consumption

The comparison shows that the device presented in this work provides in line expectations to other BLE based developments. Fulfilling the requirements of a low-power multi-sensor platform.

6. Conclusion

In this thesis, the design and implementation of a compact low-power Bluetooth Low Energy (BLE) Data Acquisition Device, with dimensions of 36.5 mm x 29.75 cm was accomplished. With this sensor node, various researchers at YSU will be able to acquire data wirelessly with few to no modifications to either the software or hardware parts of the system. Furthermore, this work also serves as a base for BLE power analysis intended to help engineers identify key functionalities for specific applications and model the performance of their designs.

The overall functionality of the BLE radio was demonstrated to be very efficient, and the Single-Ended front-end design proved to be on par with a traditionally Differential front-end design, and with a receiver sensitivity of -92.6 dBm against the differential sensitivity of -97 dBm. Such design enforces that a single-ended front end can be essential for projects and applications with restricted size and constraint budget. Also, complementing the first paragraph, there is no future need for modifications in the RF section of the hardware if not for optimization. Sensors can be added or replaced, which would only require Digital circuitry modifications.

In addition, the integration between the ADXL343 and the BME688 sensors and the BLE protocol was successfully implemented, serving as a base for the setup of the cortisol sensor present in the device. The overall current consumption, when reading and transmitting sensing data from the sensors previously mentioned were 4.1 mA and 7.1 mA respectively, considered to be of very low-power. With the CR1025 30 mAh battery chosen for the design, the sensor node can operate for 7.3 hours with only the ADXL343 on, 4.2 hours with the BME688, and combined the average lifetime of the battery with both sensors in operation is 4.35 hours. Such range intervals can be significantly increased depending on the sampling period.

Overall, the finalized PCB is of restricted size when compared to other sensor nodes like TI CC1350/CC2650 SensorTag with a total size of 60mm x 40mm, and therefore ideal for applications with space limitations.

6.1. Future Work

After completing the current design of the Data Acquisition device, a lot of possibilities for future work are opened. First, the final integration of all the sensors with BLE and embedded design improvements for efficiency and simplicity in the codes as well as the development of a Smart Device application ecosystem for data collection and analysis. On the hardware side, research can also be done to design a PCB trace 2.4 GHz antenna to substitute the chip antenna current in place, so that size optimization and cost effectiveness is achieved.

Later, research can be concluded in the optimization of the BLE stack and sensors integration, with reference from the work of *Dian et al* [9]–[11] and from *Liu et al* [12], where the power consumption is used for developing models for improved efficiency. Finally, there are a lot of opportunities for research in data security, and how BLE transactions can be improved for outside threats.

References

[1] J. Tosi, F. Taffoni, M. Santacatterina, R. Sannino, and D. Formica, "Performance evaluation of bluetooth low energy: A systematic review," *Sensors (Switzerland)*, vol. 17, no. 12. MDPI AG, Dec. 13, 2017. doi: 10.3390/s17122898.

[2] Zengtao Feng, Lingfei Mo, and Meng Li, "Analysis of low energy consumption wireless sensor with BLE," in *2015 IEEE SENSORS*, Nov. 2015, pp. 1–4. doi: 10.1109/ICSENS.2015.7370563.

[3] C. Liu, Y. Zhang, and H. Zhou, "A comprehensive study of bluetooth low energy," in *Journal of Physics: Conference Series*, Nov. 2021, vol. 2093, no. 1. doi: 10.1088/1742-6596/2093/1/012021.

[4] K. S. Burman, S. Schmidt, D. el Houssaini, and O. Kanoun, "Design and Evaluation of a Low Energy Bluetooth Sensor Node for Animal Monitoring," in *18th IEEE International Multi-Conference on Systems, Signals and Devices, SSD 2021*, Mar. 2021, pp. 971–978. doi: 10.1109/SSD52085.2021.9429390.

[5] D. Taşkın, C. Taşkın, and S. Yazar, "Developing a Bluetooth Low Energy Sensor Node for Greenhouse in Precision Agriculture as Internet of Things Application," *Advances in Science and Technology Research Journal*, vol. 12, no. 4, pp. 88–96, Dec. 2018, doi: 10.12913/22998624/100342.

[6] T. Wu, J.-M. Redoute, and M. R. Yuce, "A Wearable Wireless Medical Sensor Network System Towards Internet-of-Patients," in *2018 IEEE SENSORS*, Oct. 2018, pp. 1–3. doi: 10.1109/ICSENS.2018.8589642.

[7] T. Wu, J.-M. Redoute, and M. R. Yuce, “Live Demonstration: A Wearable Wireless Medical Sensor Network System Towards Internet-of-Patients,” in *2018 IEEE SENSORS*, Oct. 2018, pp. 1–1. doi: 10.1109/ICSENS.2018.8589897.

[8] A. Sabatini *et al.*, “Design And Development Of An Innovative Sensor System For Non-Invasive Monitoring Of Athletic Performances,” in *2019 II Workshop on Metrology for Industry 4.0 and IoT (MetroInd4.0&IoT)*, Jun. 2019, pp. 162–166. doi: 10.1109/METROI4.2019.8792863.

[9] A. Yousefi, K. Somaratne, and F. J. Dian, “Analysis of time synchronization based on current measurement for Bluetooth Low Energy (BLE),” in *2017 8th IEEE Annual Information Technology, Electronics and Mobile Communication Conference (IEMCON)*, Oct. 2017, pp. 602–607. doi: 10.1109/IEMCON.2017.8117157.

[10] F. J. Dian, A. Yousefi, and K. Somaratne, “Performance evaluation of time synchronization using current consumption pattern of BLE devices,” in *2018 IEEE 8th Annual Computing and Communication Workshop and Conference (CCWC)*, Jan. 2018, pp. 906–910. doi: 10.1109/CCWC.2018.8301666.

[11] F. J. Dian, “An Analytical Scheme For Power Consumption of Battery-Operated peripheral BLE nodes,” in *2019 IEEE 9th Annual Computing and Communication Workshop and Conference (CCWC)*, Jan. 2019, pp. 1021–1026. doi: 10.1109/CCWC.2019.8666550.

[12] C. Huang, H. Liu, W. Wang, and J. Li, “A Compact and Cost-Effective BLE Beacon with Multiprotocol and Dynamic Content Advertising for IoT Application,” *IEEE Internet Things J*, vol. 7, no. 3, pp. 2309–2320, Mar. 2020, doi: 10.1109/JIOT.2019.2958455.

[13] “https://www.altium.com/.”

[14] “https://www.ti.com/tool/CCSTUDIO.”

[15] “https://www.keysight.com/us/en/home.html.”

[16] “bst-bme688-ds000”.

[17] A. Devices, “ADXL343 (Rev. A).”

[18] “High Precision, Impedance, and Electrochemical Front End.” [Online]. Available: www.analog.com

[19] “CC13xx/CC26xx Hardware Configuration and PCB Design Considerations,” 2022. [Online]. Available: www.ti.com

[20] Brian C Wadell, “, Transmission Line Design Handbook,” 1991, p. 79.

[21] “Microstrip, Stripline, CPW, and SIW Design.” [Online]. Available: http://www.qsl.net/va3iul

[22] “https://www.bluetooth.com/blog/3-key-factors-that-determinethe-range-of-bluetooth/.”

[23] C. Gomez, J. Oller, and J. Paradells, “Overview and evaluation of bluetooth low energy: An emerging low-power wireless technology,” *Sensors (Switzerland)*, vol. 12, no. 9, pp. 11734–11753, Sep. 2012, doi: 10.3390/s120911734.

[24] M. Magno, F. Vultier, B. Szebedy, H. Yamahachi, R. H. R. Hahnloser, and L. Benini, “A Bluetooth-Low-Energy Sensor Node for Acoustic Monitoring of Small Birds,” *IEEE Sens J*, vol. 20, no. 1, pp. 425–433, Jan. 2020, doi: 10.1109/JSEN.2019.2940282.

[25] T. N. Gia *et al.*, “IoT-based fall detection system with energy efficient sensor nodes,” in *2016 IEEE Nordic Circuits and Systems Conference (NORCAS)*, Nov. 2016, pp. 1–6. doi: 10.1109/NORCHIP.2016.7792890.